JOURNAL OF BACTERIOLOGY, Sept. 1991, p. 5822–5830
0021-9193/91/185822-09$02.00/0

Vol. 173, No. 18

Cloning and Characterization of a *Rhizobium meliloti* Homolog of the *Escherichia coli* Cell Division Gene *ftsZ*

WILLIAM MARGOLIN, JOSEPH C. CORBO,† AND SHARON R. LONG*

Department of Biological Sciences, Stanford University, Stanford, California 94305-5020

Received 29 May 1991/Accepted 17 July 1991

The *ftsZ* gene is essential for initiation of cell division in *Escherichia coli* and *Bacillus subtilis*. To begin our studies of division arrest during differentiation of *Rhizobium meliloti* bacteroids, we isolated a *R. meliloti ftsZ* homolog, $ftsZ_{Rm}$. Degenerate primers directed towards a conserved region of *ftsZ* were used to amplify a segment of *R. meliloti* DNA by polymerase chain reaction, and the product of this reaction was then used to isolate positive clones from a bacteriophage library. The DNA sequence of an open reading frame containing the region of homology indicated that the *R. meliloti* FtsZ protein ($FtsZ_{Rm}$) is 50% homologous to the known *E. coli* and *B. subtilis* FtsZ proteins, but at 590 amino acids (63 kDa), it is predicted to be nearly 50% larger. Strong expression of an approximately 70-kDa labeled protein in a coupled in vitro transcription-translation system supports this prediction. The additional 200 amino acids appear to fall in a single internal domain highly enriched for proline and glutamine residues. When we regulated *R. meliloti ftsZ* ($ftsZ_{Rm}$) expression on a high-copy-number plasmid in *E. coli* with P_{lac} and $lacI^q$, cells were smaller than normal in the presence of low $FtsZ_{Rm}$ levels (with no isopropyl-β-D-thiogalactopyranoside [IPTG]) and filamentous when $FtsZ_{Rm}$ was overproduced (with IPTG). These results suggest that low levels of $FtsZ_{Rm}$ stimulate *E. coli* cell division, while high levels may be inhibitory.

During development of nitrogen-fixing nodules in alfalfa, *Rhizobium meliloti* bacteria are released from infection threads into root cortical cells and surrounded by a plant-derived peribacteroid membrane, and then they begin differentiating into bacteroids capable of fixing atmospheric nitrogen (19). Two important physiological changes that occur during differentiation are the cessation of cell division and the arrest of DNA replication after a few rounds (39). Mature bacteroids of *R. meliloti* have an increased nucleic acid content and a more rounded shape and are larger than their free-living predecessors (29). Occasional branched forms are also seen. Morphological changes during development in nonsymbiotic microbial systems such as *Bacillus subtilis* or *Caulobacter crescentus* have been well studied (20, 27), but the genes and factors involved in the morphological aspects of *Rhizobium* differentiation have not been defined. One potential way of addressing the mechanism of division arrest and bacteroid morphogenesis is to understand the genes and factors required for cell division control in *Rhizobium* cells. Since cell cycle mutants of *R. meliloti* bacteroids have not yet been isolated, our initial strategy involves isolating homologs of key *Escherichia coli* cell cycle genes that might be developmentally regulated in *R. meliloti*.

In *E. coli*, *ftsZ* is a key gene required for normal cell division (for reviews, see references 8, 15, and 21). FtsZ acts early in the cell division process, since heat induction of *ftsZ* temperature-sensitive mutant cells results in complete and immediate cessation of division (10), and the filamentous cells thus formed have no visible constriction points (4). FtsZ also appears to be rate limiting for septum initiation: moderately increasing the level of FtsZ results in a minicell phenotype because of an increase in division frequency at the cell poles, and the average cell becomes smaller, suggesting that septation is occurring earlier in the cell cycle (42). Very high levels of FtsZ, however, completely inhibit division (5, 42). FtsZ protein appears to be a target of other division factors: the products of the *minCD* locus, which appear to suppress divisions at the cell poles, act to antagonize the FtsZ effect (5). Also, SulA, which is induced during DNA damage, inhibits the effect of FtsZ, resulting in cell filamentation (21).

The *ftsZ* gene is conserved in other eubacteria, as demonstrated by Southern blot and Western blot (immunoblot) analyses (7). The only other characterized *ftsZ* homolog, from *B. subtilis*, encodes a protein that is 50% identical to *E. coli* FtsZ (2) and is essential for synthesis of both vegetative and sporulation septa (3). However, expression of *B. subtilis ftsZ* in *E. coli* inhibits host cell division (2). In this paper, we report the isolation and initial characterization of a *R. meliloti ftsZ* homolog which shares sequence similarity with its *E. coli* and *B. subtilis* counterparts and affects *E. coli* cell division but codes for a significantly larger protein than its counterparts do.

MATERIALS AND METHODS

Media, chemicals, and enzymes. Ampicillin, kanamycin, and tetracycline were used in Luria broth (32) and plates as necessary at 50, 50, and 10 μg/ml, respectively. To detect inserts in pUC or pBluescript vectors, Luria broth plates with ampicillin were supplemented with a 20-mg/ml solution of 5-bromo-4-chloro-3-indolyl-β-D-galactopyranoside and IPTG (isopropyl-β-D-thiogalactopyranoside) in *N*,*N*-dimethylformamide to give a final concentration of 40 μg/ml. Restriction enzymes, T4 DNA ligase, and Klenow DNA polymerase were from New England BioLabs or Promega Biotec and were used according to the manufacturers' recommendations. Radiochemicals were from Amersham.

Bacterial strains, bacteriophages, and plasmids. All strains and plasmids used are listed in Table 1. JFL101 was obtained from J. Lutkenhaus.

* Corresponding author.
† Present address: Soil Science Unit, Joint FAO/IAEA Programme, Seibersdorf Laboratory, A2444-Seibersdorf, Austria.

TABLE 1. Strains, phages, and plasmids used in this study

Strain, phage, or plasmid	Genotype or characteristics	Source or reference
R. meliloti		
RCR2011	Wild type	26
1021	Str^r derivative of RCR2011	26
E. coli		
XL1-blue	*recA1 endA1 gyrA96 thi hsdR17 supE44 relA1 lac* (F′ *proAB lacI*^{q}ZΔM15, Tn*10*)	32
LE392	*hsdR514 hsdM supE44 supF58* Δ(*lacIZY*)*6 galK2 galT22 metB1 trpR55*	32
pLK-17	*lac mcrA mcrB hsdR gal supE*	Stratagene
JFL101	*ftsZ84 recA ilv deo ara*(Am) *lacZ125*(Am) *galU42*(Am) *trp*(Am) *tyrT supFA81*(Ts)	J. Lutkenhaus
Bacteriophages		
λGEM-11	λ replacement-cloning vector	Promega Biotec
λJC9	λGEM-11 containing 10- and 4-kb *Bam*HI fragments from *R. meliloti* replacing central stuffer	This work
Plasmids		
pBluescript SK+	*lac* expression vector (Ap^r) containing M13 replication origin	Stratagene
pUC118	pUC18 (Ap^r) containing M13 replication origin	41
pUC119	Same as pUC118, with reversed polylinker	41
pJC8	220-bp cloned PCR product (*Eco*RI fragment)	This work
pJC05	3-kb *Xho*I fragment containing *ftsZ*$_{Rm}$	This work
pJC06	2-kb *Bam*HI-*Hin*dIII fragment containing *ftsZ*$_{Rm}$	This work
pJC18	10-kb *Bam*HI fragment containing *ftsZ*$_{Rm}$	This work
pJC062	0.22-kb deletion of C terminus of *ftsZ*$_{Rm}$	This work

PCR. Synthesis of a 221-bp polymerase chain reaction (PCR) product containing a segment of *ftsZ* from *R. meliloti* total DNA was accomplished with the following primers (Pu is a purine, Py is a pyrimidine, and N is G, A, T, or C): 5′CTTGAATTCAAPyACNGAPuGCNCAPuGC3′ (to prime synthesis of the nontemplate strand) and 3′TACCCNCCNC CNTGNCCNTGCTTAAGTTC5′ (template strand). Two segments of amino acid identity between the *B. subtilis* and *E. coli* FtsZ proteins that were spaced sufficiently far apart within the gene to give an easily detectable PCR product and that could yield relatively nondegenerate primer sequences, particularly at the 3′ ends, were chosen. At the third position in a codon, maximum degeneracy was introduced in order to prevent a complete mismatch. Annealing potential at the 3′ end was maximized by using only the first two invariant positions of the C-terminal amino acid codon. To facilitate cloning of the PCR product, we engineered the 5′ termini to contain both an *Eco*RI restriction site and a CTT terminal trinucleotide to make the site more accessible to the *Eco*RI enzyme.

PCR reactions were performed on an Ericomp programmable thermal reactor in a 0.1-ml reaction mixture containing 10 mM Tris (pH 8.3), 1.5 mM $MgCl_2$, 50 mM KCl, 0.1 mg of gelatin per ml, deoxynucleoside triphosphates at 0.2 mM, primers at 1 μM, 0.1 to 1 μg of template DNA, and 3 U of *Thermus aquaticus* DNA polymerase (Amplitaq; Perkin-Elmer/Cetus). Each of the 30 cycles of amplification consisted of denaturation for 1 min at 95°C, annealing for 1 min at 55°C, and polymerization for 2 min at 74°C. PCR products were then separated by electrophoresis on a 2% agarose gel in Tris-borate-EDTA buffer at 250 V, visualized by ethidium bromide staining and UV light, excised, eluted, and purified by extraction with phenol-chloroform and precipitation with ethanol.

Preparation and manipulation of DNA. Total genomic DNA from *R. meliloti* 1021 was prepared as described previously (26). Minipreparations of plasmid DNA from *E. coli* were done by alkaline extraction (32). Large-scale plasmid preparations for use as templates in S-30 reactions were isolated from CsCl gradients as described elsewhere (32). Minipreparations of phage λ DNA were made from high-titer liquid lysates essentially as described elsewhere (25). DNA fragments were purified either by elution from agarose gels by freeze-squeeze (40) or directly from low-melting-point GTG agarose (SeaKem) as described elsewhere (32).

Construction and screening of the phage library. A library of *R. meliloti* 1021 DNA, constructed by D. Bramhill, was made by ligating total DNA partially digested with *Bam*HI into *Bam*HI-cleaved arms of λGEM-11 according to the instructions given by Promega Biotec. The phage were plated on *E. coli* LE392 or pLK-17 to give single plaques and transferred to GeneScreen nylon membranes (New England Nuclear); phage DNA was fixed to the filters as described before (22). The filters were screened with the insert from pJC8. After positives were purified and rescreened, phage DNA from λJC9 was isolated, digested, blotted, and probed with the insert from pJC8 to map the gene.

Plasmid constructions. Plasmid pJC8 was made by ligating *Eco*RI-cleaved pUC119 to the gel-purified 221-bp PCR product which had been cleaved with *Eco*RI. Plasmids pJC18 and pJC05 were made by cloning the λJC9 10-kb *Bam*HI and 3-kb *Xho*I fragments that contained homology to the PCR product into *Bam*HI- and *Xho*I-cleaved pUC119, respectively. In plasmid pJC05, the orientation of *ftsZ* is opposite to that of the vector *lac* promoter (P_{lac}). Plasmid pJC06 was constructed by cleaving pJC05 with *Bam*HI (in the pUC119 polylinker) and *Hin*dIII (downstream of *ftsZ*) and cloning it into pBluescript cleaved with *Bam*HI and *Hin*dIII, placing *ftsZ* under the control of P_{lac}. For DNA sequencing, nested deletions from the polylinkers of pJC05 and pJC06 were made by using exonuclease III and S1 nuclease (Bethesda Research Laboratories) as previously described (32). Some parts of the sequence that were not covered by exonuclease deletions were subcloned into either pUC118 or pUC119 for sequencing. Plasmid pJC062 is an exonuclease III deletion derivative of pJC06, in which 395 nucleotides of *R. meliloti* DNA was deleted from the *Hin*dIII site.

DNA sequencing. Single-stranded DNA for sequencing was prepared from plasmids derived from pUC118, pUC119, or pBluescript SK+ by using the M13K07 helper phage as described elsewhere (31). DNA sequencing using the dideoxynucleotide chain termination method (33) was carried out with the Sequenase 2.0 kit (U.S. Biochemicals) using either the −40 primer from the kit (pJC05 derivatives) or the T7

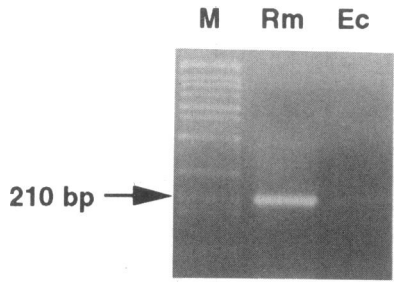

FIG. 1. Ethidium bromide-stained gel showing PCR amplification of a segment of *R. meliloti ftsZ*. A 2% agarose gel was loaded with λ DNA digested with *Bgl*I (lane M), half of a PCR reaction mixture with *R. meliloti* DNA template (lane Rm), and half of a PCR reaction mixture with *E. coli* DNA template (lane Ec). The arrow denotes the position of the 210-bp marker.

promoter primer from Promega Biotec (pJC06 derivatives). Both dGTP and dITP mixes were used.

In vitro protein synthesis. Coupled transcription-translation reactions contained S-30 extracts made from *R. meliloti* RCR2011 and 1 μg of the appropriate CsCl-banded plasmid DNA template and were performed as described previously (11). Proteins labeled with [^{35}S]methionine were diluted in sample buffer, separated by sodium dodecyl sulfate-polyacrylamide gel electrophoresis (17), and visualized by autoradiography using Kodak XAR-5 film.

DNA sequence analysis. DNA and protein sequence comparisons, characterizations, and mapping were done with the University of Wisconsin Genetics Computer Group programs (9). Data base homology searches were done with FASTA and TFASTA (18). Multiple sequence alignments were accomplished with TULLA (38).

Microscopic techniques. Bacterial cells grown in Luria broth with ampicillin were placed directly on glass slides without fixation and viewed under a Nikon light microscope with Nomarski optics. Photographs were taken with a Nikon FE 35-mm camera and Kodak Ektachrome (160 ASA) film.

RESULTS

Cloning the *ftsZ*$_{Rm}$ gene. Since the DNA sequence homology between the *E. coli* and *B. subtilis ftsZ* genes is only 50% (2) and since *Rhizobium* DNA has a much higher GC content, we did not expect to easily detect the *R. meliloti* homolog by Southern hybridization using an internal segment of the *E. coli ftsZ* gene as a probe. However, there are many short segments of amino acid identity between the *E. coli* and *B. subtilis* FtsZ proteins. We reasoned that a PCR approach using primers to these regions would successfully amplify internal *R. meliloti*-specific sequences that could be used as a 100% homologous probe to screen a genomic library. Therefore, primers corresponding to two relatively nondegenerate hexamer amino acid segments near the N terminus which would give rise to a predicted 221-bp PCR product were made (see Materials and Methods). After amplification of *R. meliloti* 1021 genomic DNA with these primers, a 221-bp product, which was by far the predominant species, was observed (Fig. 1). This product was cloned into pUC119 to make pJC8.

The DNA sequence of the cloned PCR product (pJC8) revealed a partial reading frame coding for 68 amino acids with 57% amino acid identity to *E. coli* FtsZ (FtsZ$_{Ec}$) and 62% identity to *B. subtilis* FtsZ (FtsZ$_{Bs}$), indicating that a portion of the *R. meliloti ftsZ* gene had been successfully amplified. The GC-rich DNA sequence of the pJC8 insert was only 57 and 63% homologous to the corresponding regions in *ftsZ*$_{Ec}$ and *ftsZ*$_{Bs}$, respectively, suggesting that a hybridization approach would have been difficult. The DNA sequence of the amplified fragment also revealed closely spaced *Pst*I and *Nsi*I sites that would subsequently prove useful in locating *ftsZ* on a λ clone and determining its orientation.

As expected, the amplified region hybridized much more strongly to *R. meliloti* DNA than to *E. coli* DNA on a Southern blot; consequently, it was used to screen a λ library of *R. meliloti* DNA. Several positive clones were obtained; one, λJC9 (Fig. 2), which contained a 10-kb *Bam*HI insert which hybridized to the probe, was chosen for further study. Southern blot analysis of restriction enzyme-digested *R. meliloti* genomic DNA and purified λJC9 DNA indicated that the entire *ftsZ* gene was probably contained within the *Bam*HI insert, based on the predicted position of the PCR product within the coding region and the mapped location of this PCR product within the *Bam*HI fragment (Fig. 2). A 3-kb *Xho*I fragment likely containing the entire *ftsZ*$_{Rm}$ gene was subcloned (pJC05); it and another 2-kb *Bam*HI-*Hin*dIII subclone with the insert in the opposite orientation (pJC06) were used for DNA sequencing (Fig. 2).

DNA and deduced protein sequence analysis of *ftsZ*. We obtained the nucleotide sequence of the 2-kb *Bam*HI-*Hin*dIII fragment on both DNA strands by using the strategy diagrammed in Fig. 2. The sequence (Fig. 3) revealed a single long open reading frame coding for an acidic 590-amino-acid protein, predicted to be 63.0 kDa with an isoelectric point of 4.91. This *ftsZ*$_{Rm}$ reading frame uses a high percentage of preferred *R. meliloti* codons throughout its entire length (1) and is preceded by a sequence highly homologous to the Shine-Dalgarno sequence important for ribosome binding (Fig. 3, underlined), suggesting that it is translated efficiently (36). An inverted repeat resembling a stable rho-independent terminator structure (30) lies 130 to 150 bp downstream from the stop codon, having a calculated ΔG of approximately −17 kcal (1 cal = 4.184 J) (12) (Fig. 3).

The FtsZ$_{Rm}$ protein is 45 to 50% identical to both the *B. subtilis* and the *E. coli* FtsZ proteins; a three-way protein alignment is shown in Fig. 4. A pairwise comparison of the three proteins gives comparable levels of relatedness. Strikingly, however, the predicted 590-amino-acid *R. meliloti* FtsZ protein is more than 50% larger than FtsZ$_{Ec}$ (383 residues) and FtsZ$_{Bs}$ (382 residues). In this alignment, the extra approximately 200 amino acids in FtsZ$_{Rm}$ are present in a single nonhomologous domain near the C terminus (Fig. 4). All three proteins have similar amino acid compositions; however, FtsZ$_{Rm}$ contains 8.1% proline residues versus 3.92% in FtsZ$_{Ec}$ and 3.40% in FtsZ$_{Bs}$ (Table 2). The nonhomologous domain in FtsZ$_{Rm}$ is especially enriched in proline and glutamine residues, which together account for over 30% of the total amino acids in this region (Table 2). In fact, when 202 amino acids from this region are removed from the FtsZ$_{Rm}$ sequence, the size, charge, and composition of this deleted protein (Table 2) become very similar to those of FtsZ$_{Ec}$ and FtsZ$_{Bs}$; the only exception is the presence in FtsZ$_{Rm}$ of three cysteine residues, while the other FtsZ proteins lack cysteines.

We searched the data base for proteins with potential homology to FtsZ$_{Rm}$ but found no proteins other than FtsZ$_{Ec}$ and FtsZ$_{Bs}$ with significant sequence similarity. However, when the 200-amino-acid nonhomologous domain of FtsZ$_{Rm}$ was used to search the data base, among the proteins receiving the highest similarity scores were several wheat

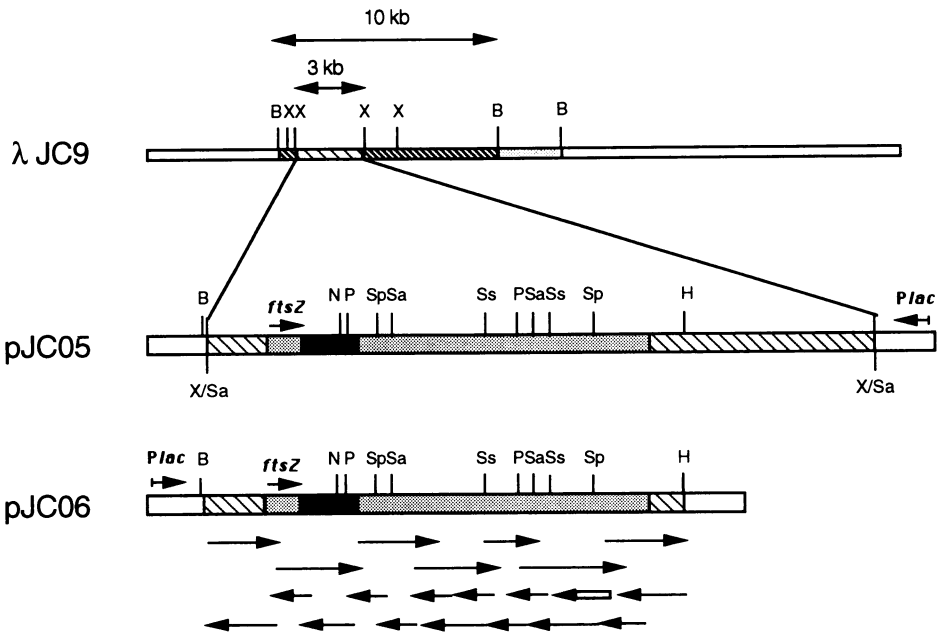

FIG. 2. Restriction nuclease map and sequencing strategy for the *R. meliloti ftsZ* gene. Narrow open boxes denote λGEM-11 DNA arms; filled boxes denote cloned *R. meliloti* DNA inserted into the *Bam*HI site. These include the 3-kb *Xho*I fragment and the 10-kb *Bam*HI fragment that hybridize to the *ftsZ* PCR product probe (lightly and densely hatched boxes, respectively) and another *Bam*HI insert that does not hybridize to the *ftsZ* probe (stippled box). Thick boxes denote portions of plasmid DNA flanking the inserted *Rhizobium* DNA. These include DNA from pUC119 and pBluescript SK+ vectors (open boxes for pJC05 and pJC06, respectively), the *ftsZ* gene open reading frame (light stippled boxes), the segment of *ftsZ* represented by the PCR product (dark stippled boxes), and the flanking segments of cloned *R. meliloti* DNA (hatched areas). The orientation of *ftsZ* and the vector *lac* promoters (P_{lac}) are indicated by arrows above the boxes. The sequencing strategy is indicated at the bottom; the arrows represent 5′-to-3′ sequencing runs with single-stranded DNA generated by exonuclease III deletions of pJC05 (rightward arrows) or pJC06 (leftward arrows) or by subcloning into pUC119 or pBluescript SK+. The right end of the open arrow represents the extent of the deletion in pJC062. Restriction endonuclease cleavage sites are represented by vertical tick marks: B, *Bam*HI; H, *Hin*dIII; N, *Nsi*I; P, *Pst*I; Sa, *Sal*I; Sp, *Sph*I; Ss, *Sst*I; X, *Xho*I.

high-molecular-weight glutenins, which contain extensive proline-glutamine tracts that resemble the Pro-Gln motifs found in $FtsZ_{Rm}$.

In view of the possibility that the 200-amino-acid domain had originated by an insertion event or had been removed in *E. coli* and *B. subtilis* by a splicing event, perhaps analogous to σ^k processing in *B. subtilis* (37), we searched for potential splice sites and inverted repeats flanking the domain. A 7-base inverted repeat (TCGTCGC; Fig. 3) was found; the left repeat was located 11 nucleotides upstream from the start of the nonhomologous domain, while the right repeat was located at the C-terminal boundary of the domain. However, neither this sequence nor any potential splicing sequences were found in the other homologs, so the significance of the inverted repeat is unclear.

Detection of FtsZ protein. Previous observations by Corton et al. (7) support the prediction that $FtsZ_{Rm}$ protein is much larger than its homologs: a protein from *Agrobacterium tumefaciens*, a close relative of *R. meliloti* (43), was shown to migrate at a significantly higher molecular mass than *E. coli* FtsZ on a Western blot probed with anti-FtsZ antiserum (7). To further test the idea that $FtsZ_{Rm}$ is much larger than its *E. coli* and *B. subtilis* counterparts, we expressed [^{35}S] methionine-labeled $FtsZ_{Rm}$ in a *R. meliloti*-derived cell-free transcription-translation system (S-30 extract). When the full-length $ftsZ_{Rm}$ gene was used as template, a tight triplet of bands migrating with an apparent molecular mass of approximately 70 kDa was strongly expressed (Fig. 5). The degree of expression was independent of whether $ftsZ_{Rm}$ was in the same orientation as P_{lac} (pJC06) or in the opposite orientation (pJC05). This apparent size is 7 kDa larger than the predicted 63 kDa, which may be a result of aberrant migration, as has been observed with other acidic proteins such as bacterial σ factors (14). To demonstrate that this triplet represents $FtsZ_{Rm}$, a template was used (pJC062) that lacks the last 72 amino acids of $FtsZ_{Rm}$ and has a reading frame terminating 2 amino acids into the pUC119 polylinker, resulting in a 520-amino-acid protein predicted to be approximately 8 kDa smaller than the wild-type $FtsZ_{Rm}$ (Fig. 2). A triplet migrating with an apparent molecular mass of approximately 62 kDa was indeed observed (Fig. 5), strongly suggesting that the triplet represents $FtsZ_{Rm}$. The fact that the truncated species also migrates unusually slowly suggests that the features that cause aberrant migration are still intact in the truncated species; this idea is supported by the estimated isoelectric point of the truncated protein of 4.74, which is similar to that of the full-length protein.

To provide additional support for the existence of an unusually large *R. meliloti* FtsZ protein, we carried out Western analysis of $FtsZ_{Rm}$ synthesized from plasmids in *E. coli* with anti-$FtsZ_{Ec}$ serum (7). In addition to the 40-kDa $FtsZ_{Ec}$ band, a band at approximately 70 to 80 kDa was visible on a blot containing protein from strain XL1-Blue (*lacI*^{q}) carrying plasmid-borne $ftsZ_{Rm}$ under P_{lac} control (pJC06) and became at least 10 times more intense with protein from the same strain after induction with 1 mM IPTG over 24 h (results not shown). Multiple bands were not observed; this lack could be due either to the presence of

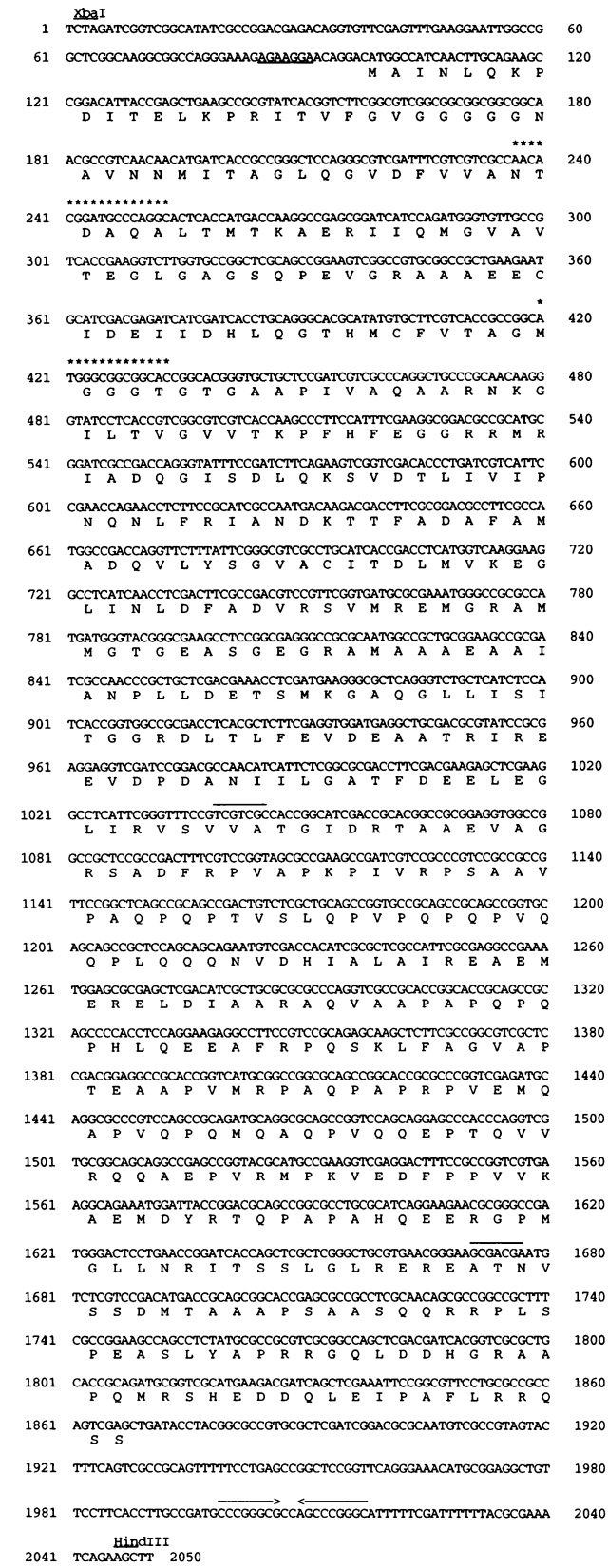

FIG. 3. Nucleotide and predicted protein sequences of the *R. meliloti ftsZ* gene. The sequence of the nontemplate strand is shown from an *Xba*I site 92 bases within the pJC05-pJC06 insert from the *Xho*I site to the *Hin*dIII site; the sequence is numbered starting with the 5′-terminal base in the *Xba*I recognition sequence. The amino acid sequence is shown in single-letter code, with each letter below the first base of its corresponding codon; the period denotes a termination codon. The underlined sequence is the predicted ribosome-binding site. The inverted arrows represent inverted repeats which are part of a predicted rho-independent terminator stem. Asterisks above the sequence denote the bases to which PCR primers were directed. Solid lines above the sequence mark the positions of the TCGTCGC inverted repeats.

only one immunoreactive species or to the inability of this method to resolve the triplet bands. Although the antibody did not appear to be specific enough to detect a 70- to 80-kDa band above background from *R. meliloti* 1021 total protein, the IPTG-inducible 70- to 80-kDa band in *E. coli* is consistent with the size observed in vitro.

Effects of $FtsZ_{Rm}$ expression on *E. coli* growth and cell division. In order to determine whether the cloned $ftsZ_{Rm}$ exhibited biological activity, we assayed the effects of the cloned gene on *E. coli* cells. The presence of $ftsZ_{Rm}$ on a high-copy-number pUC derivative (pJC05) in strain XL1-Blue was not detrimental to *E. coli* growth or viability (data not shown), and cell morphology appeared to be similar to that of XL1-Blue cells containing pBluescript vector (Fig. 6a). *E. coli* XL1-Blue cells containing $lacI^q$ and $ftsZ_{Rm}$ under the control of P_{lac} (pJC06) had severalfold-lower levels of FtsZ than those containing pJC05, as assayed by Western blot (results not shown). Microscopic analysis revealed that the average length of these cells was much less than that of cells containing pJC05 or pBluescript vector (Fig. 6b), suggesting that low-level expression of $FtsZ_{Rm}$ results in hyperdivision. However, induction of these cells carrying pJC06 with 1 mM IPTG led to cell filamentation (Fig. 6d) and at least a 10-fold decrease in CFU after 24 h (data not shown), suggesting that the overproduced $FtsZ_{Rm}$ was directly or indirectly inhibiting the *E. coli* cell division system. We reasoned that intermediate levels of expression might result in a phenotype between the small-cell and filamentous phenotypes. This idea was supported by the appearance of mostly normal-length cells at IPTG concentrations between 1 and 10 μM, suggesting that an equilibrium had been reached between division stimulation and inhibition (Fig. 6c). Neither pJC06 nor pJC05 was able to complement the *ftsZ84*(Ts) mutation in JFL101, which results in filamentation at high temperature (data not shown); however, JFL101 does not have the $lacI^q$ allele and thus might allow a significantly higher level of $ftsZ_{Rm}$ expression than the XL1-Blue derivatives used in the procedures described above.

DISCUSSION

In *E. coli*, the *ftsZ* gene is essential for initiation of the division septum, the first known step in the separation of two bacterial cells. As a first step in our effort to understand the mechanism of division arrest during bacteroid differentiation, we have isolated a *R. meliloti ftsZ* homolog by using PCR to obtain a completely homologous probe internal to the gene. The high degree of amino acid identity shared between the *E. coli* and *B. subtilis* proteins facilitated the PCR approach, which was simple and rapid and allowed identification of definite *ftsZ* sequence homology before a library was searched. The sequences of only two *ftsZ* genes were known prior to this work. The PCR was successful since the amino acids in the region of the primers are

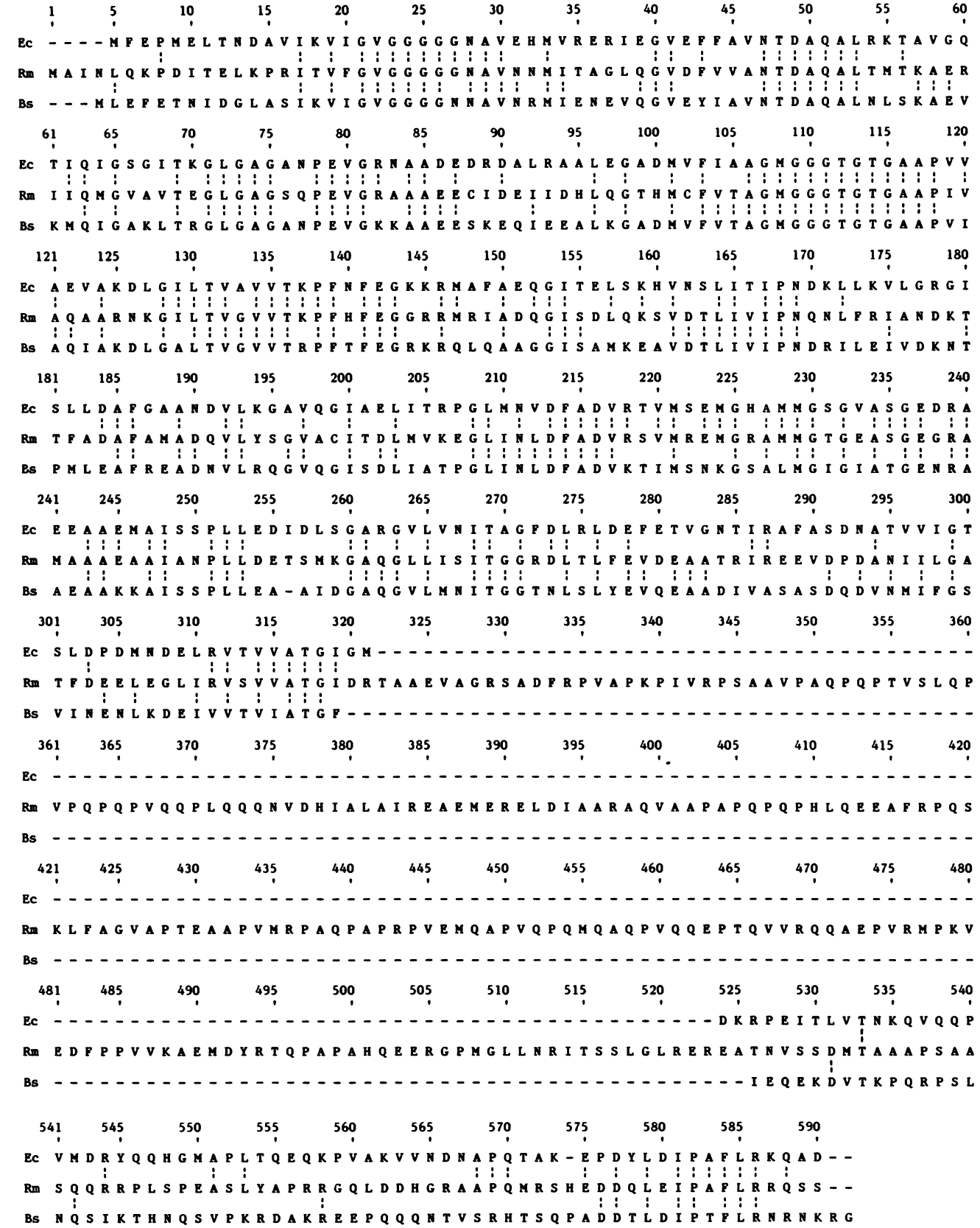

FIG. 4. Amino acid sequence alignment of FtsZ proteins from *E. coli* ($FtsZ_{Ec}$), *R. meliloti* ($FtsZ_{Rm}$), and *B. subtilis* ($FtsZ_{Bs}$), indicated by Ec, Rm, and Bs, respectively. Identical amino acids in $FtsZ_{Rm}$ and at least one of the others at a given position are marked with vertical dashes. The numbering system is relative to the $FtsZ_{Rm}$ sequence.

TABLE 2. Properties and composition of known FtsZ proteins and $FtsZ_{Rm}$ domains[a]

Property	$FtsZ_{Rm}$	$FtsZ_{Ec}$	$FtsZ_{Bs}$	$FtsZ_{Rm}$-ext[b]	$FtsZ_{Rm}$-int[c]
Mol wt	62,974	40,297	40,355	40,895	22,097
Net charge	−18	−18	−10	−17	−1
pI	4.91	4.54	4.84	4.61	6.82
No. of residues	590	383	382	388	202
Mol% of [d]:					
Ala	13.9	12.3	11.5	13.4	14.9
Gly	7.8	11.0	10.0	10.6	2.5
Cys	0.5	0.0	0.0	0.8	0.0
Ile	5.4	5.7	8.2	7.0	2.5
Leu	6.4	7.6	7.1	7.2	5.0
Val	8.0	9.9	8.1	7.0	9.9
Met	4.1	4.2	2.9	4.4	3.5
Phe	2.7	3.4	2.4	3.1	2.0
Tyr	0.5	0.5	0.5	0.5	0.5
Trp	0.0	0.0	0.0	0.0	0.0
Pro	8.1	3.9	3.4	3.6	16.8
Gln	7.8	3.7	5.2	4.6	13.9
Asn	2.5	4.4	6.3	3.4	1.0
Arg	7.0	4.7	4.2	6.4	7.9
Lys	2.2	4.4	6.0	2.3	2.0
Glu	7.0	6.8	7.3	6.4	7.9
Asp	5.3	7.1	5.5	6.7	2.5
His	1.4	1.0	0.5	1.3	1.5
Ser	4.1	3.1	4.7	4.6	3.0
Thr	5.4	6.3	6.3	6.7	3.0

[a] Values in this table were obtained from the PEPTIDESORT program.
[b] Compilation of amino acids 1 to 321 and 524 to 590 of $FtsZ_{Rm}$.
[c] Compilation of amino acids 322 to 523 of $FtsZ_{Rm}$.
[d] Values rounded to the nearest 10th.

completely conserved in all three bacteria, and the degeneracies within the primer sequences allowed for the changes at the DNA level.

The $FtsZ_{Rm}$ protein has over 200 amino acids more than its homologs, and they appear to be in a single nonhomologous domain. The weak amino acid sequence similarity to wheat prolamin storage proteins is due to the predominance of proline and glutamine repeats in the glutenins. It has been proposed that these repeats form a stacked β-sheet secondary structure which could account for the mechanical flexibility of these glutenous proteins (35). However, Chou-Fasman secondary structure predictions for this region of $FtsZ_{Rm}$ do not predict an obvious β structure (24), leaving the possible role of this region unclear at present. The 7-bp inverted repeats that flank the region hint at the possibility of an insertion event giving rise to this domain, but the domain is not homologous to any insertion elements in the data base, so the evolutionary origins of this sequence remain uncertain.

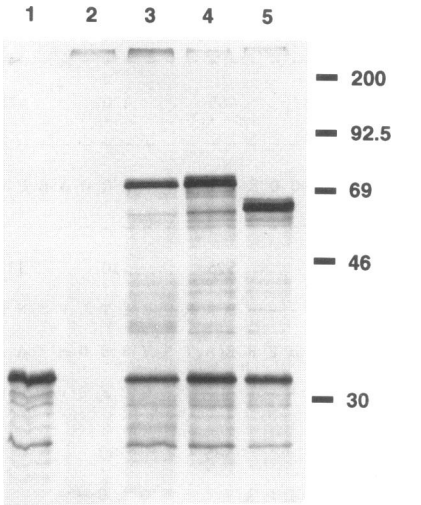

FIG. 5. Synthesis of $FtsZ_{Rm}$ in vitro. Shown is an autoradiograph of a sodium dodecyl sulfate-polyacrylamide gel loaded with [^{35}S]methionine-labeled protein from a *R. meliloti* S-30 extract primed with the following DNA templates: pBluescript SK+ (lane 1), no DNA (lane 2), pJC05 (lane 3), pJC06 (lane 4), and pJC062 (lane 5). The positions of ^{14}C-labeled protein standards are indicated at the right (in kilodaltons).

When the 200 extra amino acids of $FtsZ_{Rm}$ are not included in protein comparisons, $FtsZ_{Rm}$ is highly similar to its homologs. One exception is that $FtsZ_{Rm}$ contains cysteine residues completely lacking in the other two proteins which could be involved in disulfide cross bridges. Interestingly, the C-terminal 65 amino acids of $FtsZ_{Ec}$ and $FtsZ_{Bs}$ contain unusually high percentages of proline and glutamine residues (respectively 13.8 and 10.8% for $FtsZ_{Ec}$ and 12.3 and 9.2% for $FtsZ_{Bs}$) relative to the 3 to 5% compositions for the proteins as a whole (Table 2), suggesting that this domain may have a structural motif which is greatly expanded in the glutamine- and proline-rich nonhomologous domain of $FtsZ_{Rm}$.

Efficient expression of the *ftsZ*$_{Rm}$ gene in the *R. meliloti* S-30 extract in either orientation with respect to P_{lac} is consistent with the predicted efficient codon usage and good ribosome-binding site and suggests that a promoter for *ftsZ*$_{Rm}$ lies within the upstream 190 bp present in both pJC05 and pJC06. It is not clear why multiple protein bands were seen. There are no alternative translation initiation sites (ATG or GTG) in the sequence upstream of the *ftsZ* open reading frame, making multiple starts unlikely. Differential C termini are very unlikely, since the same pattern of bands was observed with the protein truncated at its C terminus (24). Degradation, specific processing, or modifications are still open possibilities and can be tested. Western analysis with an antibody specific for $FtsZ_{Rm}$ is the best way to investigate whether this phenomenon is seen with proteins synthesized in vivo. A considerable number of smaller bands had been observed on Western blots with FtsZ proteins from bacteria closely related to *E. coli* (7), and an analogous pattern, including the triplet band seen in vitro, could be detectable with a specific antibody. The slower mobility of $FtsZ_{Rm}$ relative to its predicted molecular weight could be due to its low pI, as is the case with σ factors, or to an unusual structure or folding pattern. It is notable that an unusual structure is postulated to be the cause of aberrantly slow migration of the high-molecular-weight wheat glutenins (13), which, as already noted, have sequence compositions similar to that of the nonhomologous domain of $FtsZ_{Rm}$.

With the *R. meliloti ftsZ* gene now cloned, the next step is to determine its possible role in septum initiation in *Rhizobium* species. Several of our findings argue that this gene is equivalent to the known *E. coli ftsZ*. First, expression of the gene is predicted to be efficient, and we observed strong in vitro expression. Second, *ftsZ*$_{Rm}$ maps physically to the large chromosome (24), which is the location of most of the housekeeping functions. Third, a reading frame homologous to *ftsA*, another essential cell division gene located immediately upstream from *ftsZ* in *E. coli* and *B. subtilis*, similarly lies just upstream from *ftsZ* in *R. meliloti* (23). Finally, an

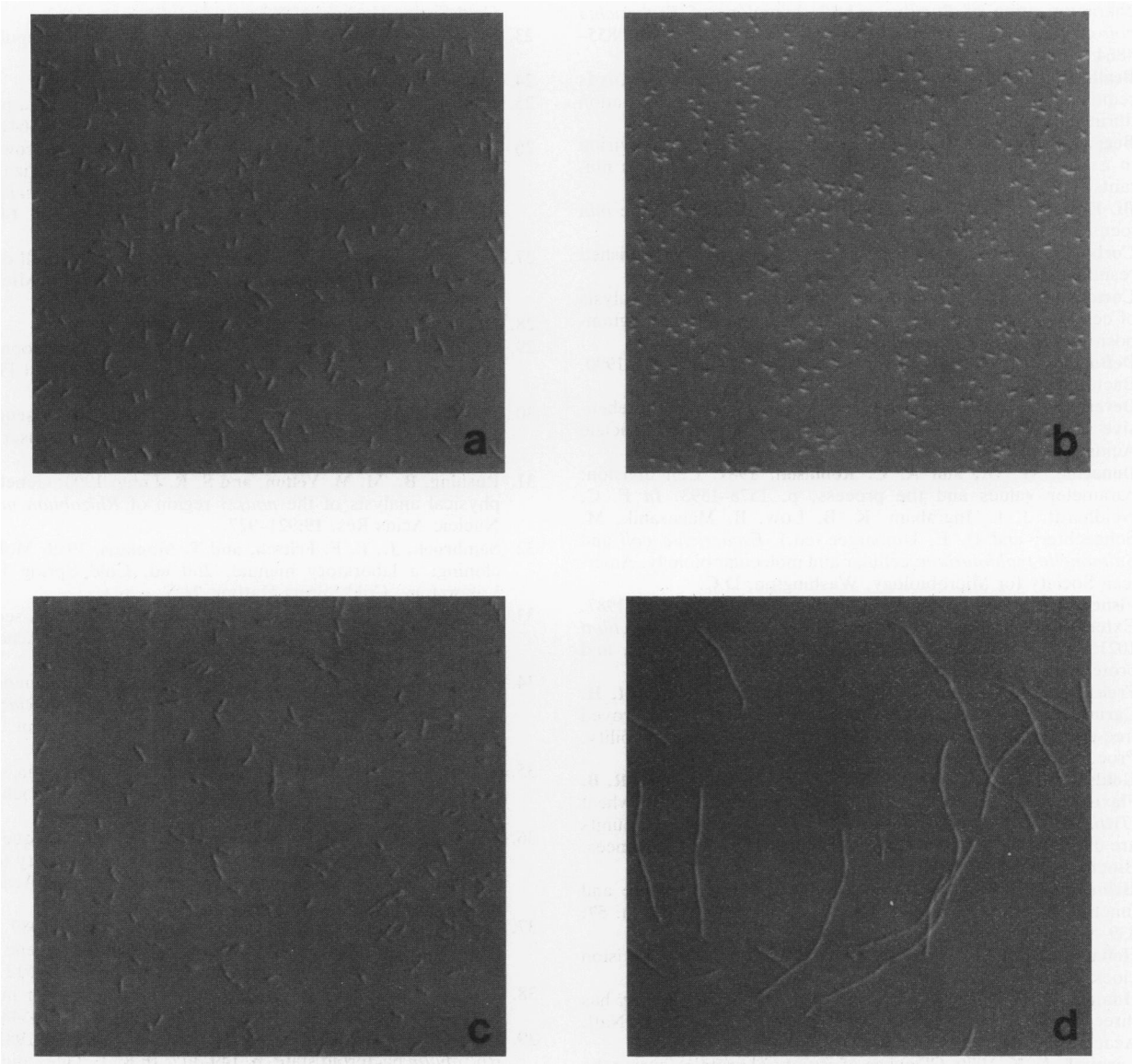

FIG. 6. *E. coli* cells (XL1-Blue) containing pBluescript vector and 1 mM IPTG (a), pJC06 with no IPTG (b), pJC06 and 10 μM IPTG (c), and pJC06 with 1 mM IPTG (d). Magnification, ×530.

IPTG dependence phenotype for $ftsZ_{Rm}$, which seems to reflect complementation at low levels and division inhibition at high levels, both consistent with a functional *ftsZ* gene, has been demonstrated in *E. coli*. However, the situation in *Rhizobium* species may be complicated. For example, several lines of evidence suggest that a second copy of $ftsZ_{Rm}$ may exist. First, weak but discrete secondary bands were observed on Southern blots containing *R. meliloti* genomic DNA probed with the cloned PCR product (6). Second, there are precedents in *R. meliloti* for duplication of genes: there exist multiple homologs of genes involved in nodulation, such as the *nodD* family (16) and the duplicate *nodPQ* locus (34); in addition, there exist two copies of a chaperonin 60 (*cpn60*) gene, which is homologous to the essential *groEL* gene of *E. coli* (28). Third, in addition to the large cross-reactive band on the Western blot of *Agrobacterium* proteins reported by Corton et al. (7), there is an equally strong band slightly smaller than 40 kDa, suggesting the presence of a second FtsZ product. Experiments addressing whether the $ftsZ_{Rm}$ gene is essential in *R. meliloti*, what effect its expression has on cell division, and whether a second $ftsZ_{Rm}$ gene exists are in progress.

ACKNOWLEDGMENTS

We thank J. Lutkenhaus for strain JFL101 and for the anti-FtsZ serum, D. Bramhill for the *R. meliloti* genomic library, and T. Egelhoff, M. Yelton, and R. Fisher for the S-30 extracts. We thank our entire group for useful discussions, and we particularly acknowledge R. Fisher, J. Ogawa, and J. Schwedock for critically reading the manuscript.

This research was supported by USDA grant 88-37262-3978. W.M. was additionally supported by an NSF Postdoctoral Fellowship in Plant Biology.

REFERENCES

1. **Barnett, M. L., and S. R. Long.** Unpublished results.
2. **Beall, B., M. Lowe, and J. Lutkenhaus.** 1988. Cloning and

characterization of *Bacillus subtilis* homologs of *Escherichia coli* cell division genes *ftsZ* and *ftsA*. J. Bacteriol. **170**:4855–4864.
3. **Beall, B., and J. Lutkenhaus.** 1991. FtsZ in *Bacillus subtilis* is required for vegetative septation and for asymmetric septation during sporulation. Genes Dev. **5**:447–455.
4. **Begg, K. J., and W. D. Donachie.** 1985. Cell shape and division in *Escherichia coli*: experiments with shape and division mutants. J. Bacteriol. **163**:615–622.
5. **Bi, E., and J. Lutkenhaus.** 1990. Interaction between the *min* locus and *ftsZ*. J. Bacteriol. **172**:5610–5616.
6. **Corbo, J. C., W. Margolin, and S. R. Long.** Unpublished results.
7. **Corton, J. C., J. J. E. Ward, and J. Lutkenhaus.** 1987. Analysis of cell division gene *ftsZ* (*sulB*) from gram-negative and gram-positive bacteria. J. Bacteriol. **169**:1–7.
8. **DeBoer, P. A. J., W. R. Cook, and L. I. Rothfield.** 1990. Bacterial cell division. Annu. Rev. Genet. **24**:249–274.
9. **Devereux, J., P. Haeberli, and O. Smithies.** 1984. A comprehensive set of sequence analysis programs for the VAX. Nucleic Acids Res. **12**:387–395.
10. **Donachie, W. D., and A. C. Robinson.** 1987. Cell division: parameter values and the process, p. 1578–1593. *In* F. C. Neidhardt, J. L. Ingraham, K. B. Low, B. Magasanik, M. Schaechter, and H. E. Umbarger (ed.), *Escherichia coli* and *Salmonella typhimurium*: cellular and molecular biology. American Society for Microbiology, Washington, D.C.
11. **Fisher, R. F., J. Swanson, J. T. Mulligan, and S. R. Long.** 1987. Extended region of nodulation genes in *Rhizobium meliloti* 1021. II. Nucleotide sequence, transcription start sites, and protein products. Genetics **117**:191–201.
12. **Freier, S. M., R. Kierzek, J. A. Jaeger, N. Sugimoto, M. H. Caruthers, T. Neilson, and D. H. Turner.** 1986. Improved free-energy parameters for predictions of RNA duplex stability. Proc. Natl. Acad. Sci. USA **83**:9373–9377.
13. **Goldsborough, A. P., N. J. Bullied, R. B. Freedman, and R. B. Flavell.** 1989. Conformational differences between two wheat (*Triticum aestivum*) 'high-molecular weight' glutenin subunits are due to a short region containing six amino acid differences. Biochem. J. **263**:837–842.
14. **Helmann, J. D., and M. J. Chamberlin.** 1988. Structure and function of bacterial sigma factors. Annu. Rev. Biochem. **57**: 839–872.
15. **Holland, I. B.** 1987. Genetic analysis of the *E. coli* division clock. Cell **48**:361–362.
16. **Honma, M., and F. M. Ausubel.** 1987. *Rhizobium meliloti* has three functional copies of the *nodD* regulatory gene. Proc. Natl. Acad. Sci. USA **84**:8558–8562.
17. **Laemmli, U. K.** 1970. Cleavage of structural proteins during the assembly of the head of bacteriophage T4. Nature (London) **227**:680–685.
18. **Lipman, D. J., and W. R. Pearson.** 1985. Rapid and sensitive protein similarity searches. Science **227**:1435–1441.
19. **Long, S. R.** 1989. *Rhizobium*-legume nodulation: life together in the underground. Cell **56**:203–214.
20. **Losick, R., P. Youngman, and P. J. Piggot.** 1986. Genetics of endospore formation in *B. subtilis*. Annu. Rev. Genet. **20**:625–669.
21. **Lutkenhaus, J.** 1990. Regulation of cell division in *E. coli*. Trends Genet. **6**:22–25.
22. **Maniatis, T., E. F. Fritsch, and J. Sambrook.** 1982. Molecular cloning: a laboratory manual. Cold Spring Harbor Laboratory, Cold Spring Harbor, N.Y.
23. **Margolin, W., J. C. Corbo, and S. R. Long.** Unpublished results.
24. **Margolin, W., and S. R. Long.** Unpublished results.
25. **Mathee, K., and M. M. Howe.** 1990. Identification of a positive regulator of the Mu middle operon. J. Bacteriol. **172**:6641–6650.
26. **Meade, H. M., S. R. Long, G. B. Ruvkun, S. E. Brown, and F. M. Ausubel.** 1982. Physical and genetic characterization of symbiotic and auxotrophic mutants of *Rhizobium meliloti* induced by transposon Tn*5* mutagenesis. J. Bacteriol. **149**:114–122.
27. **Newton, A., and N. Ohta.** 1990. Regulation of the cell division cycle and differentiation in bacteria. Annu. Rev. Microbiol. **44**:689–719.
28. **Ogawa, J., and S. R. Long.** Unpublished results.
29. **Paau, A. S., J. R. Cowles, and D. Raveed.** 1978. Development of bacteroids in alfalfa (*Medicago sativa*) nodules. Plant Physiol. **62**:526–530.
30. **Rosenberg, M., and D. Court.** 1979. Regulatory sequences involved in the promotion and termination of transcription. Annu. Rev. Genet. **13**:319–353.
31. **Rushing, B., M. M. Yelton, and S. R. Long.** 1990. Genetic and physical analysis of the *nodD3* region of *Rhizobium meliloti*. Nucleic Acids Res. **19**:921–927.
32. **Sambrook, J., E. F. Fritsch, and T. Maniatis.** 1989. Molecular cloning: a laboratory manual, 2nd ed. Cold Spring Harbor Laboratory, Cold Spring Harbor, N.Y.
33. **Sanger, F., S. Nicklen, and A. R. Coulson.** 1977. DNA sequencing with chain-terminating inhibitors. Proc. Natl. Acad. Sci. USA **74**:5463–5467.
34. **Schwedock, J., and S. R. Long.** 1989. Nucleotide sequence and protein products of two new nodulation genes of *Rhizobium meliloti*, *nodP* and *nodQ*. Mol. Plant-Microbe Interact. **2**:181–194.
35. **Shewry, P. R., and A. S. Tatham.** 1990. The prolamin storage proteins of cereal seeds: structure and evolution. Biochem. J. **267**:1–12.
36. **Shine, J., and L. Dalgarno.** 1974. The 3′-terminal sequence of *Escherichia coli* 16S ribosomal RNA: complementarity to nonsense triplets and ribosome binding sites. Proc. Natl. Acad. Sci. USA **71**:1342–1346.
37. **Stragier, P., B. Kunkel, L. Kroos, and R. Losick.** 1989. Chromosomal rearrangement generating a composite gene for a developmental transcription factor. Science **243**:507–512.
38. **Subbiah, S., and S. C. Harrison.** 1989. A method for multiple sequence alignment with gaps. J. Mol. Biol. **209**:539–548.
39. **Sutton, W. D., C. E. Pankhurst, and A. S. Craig.** 1981. The *Rhizobium* bacteroid state, p. 149–177. *In* K. L. Giles and A. G. Atherly (ed.), Biology of the Rhizobiaceae. Academic Press, Inc., New York.
40. **Tautz, D., and M. Renz.** 1983. An optimized freeze-squeeze method for the recovery of DNA fragments from agarose gels. Anal. Biochem. **132**:14–19.
41. **Vieira, J., and J. Messing.** 1987. Production of single stranded plasmid DNA. Methods Enzymol. **153**:3–11.
42. **Ward, J. E., and J. Lutkenhaus.** 1985. Overproduction of FtsZ induces minicells in *E. coli*. Cell **42**:941–949.
43. **Young, J. P. W., H. L. Downer, and B. D. Eardly.** 1991. Phylogeny of the phototrophic *Rhizobium* strain BTAi1 by polymerase chain reaction-based sequencing of a 16S rRNA gene segment. J. Bacteriol. **173**:2271–2277.